JOM 23798

Dynamic behaviour of octahedral complexes of manganese(I). X-Ray crystal structure of *fac*-[Mn(η^1-1,8-naphthyridine)-η^2-1,8-naphthyridine)$(CO)_3$]$ClO_4 \cdot CH_2Cl_2$

María-José Bermejo [a], José-Ignacio Ruiz [a], Xavier Solans [b] and Jordi Vinaixa [a]

[a] *Departament de Química Inorgànica, Universitat de Barcelona, Diagonal 647, 08028 Barcelona (Spain)*
[b] *Departament de Cristal·lografia, Mineralogía i Dipòsits Minerals, Universitat de Barcelona, Diagonal 647, 08028 Barcelona (Spain)*

(Received February 22, 1993)

Abstract

The addition of 1,8-naphthyridine (naph) to a solution of [Mn$(OClO_3)$(naph)$(CO)_3$] at room temperature affords the octahedral complex [Mn(η^1-naph)(η^2-naph)$(CO)_3$]ClO_4 (**1**). This complex can also be obtained when naph is added to a solution of [Mn$(OClO_3)(CO)_5$]. When naph is reacted with [Mn$(OClO_3)(CO)_5$] at −80°C and with 1:1 molar ratio, [Mn(η^1-naph)$(CO)_5$]ClO_4 (**3**) is obtained. This complex changes into (**1**) at temperatures above 0°C. The crystal structure of [Mn(η^1-naph)(η^2-naph)$(CO)_3$]ClO_4 (monoclinic, space group $P2_1/a$, $a = 16.006(3)$ Å, $b = 12.024(2)$ Å, $c = 13.004(2)$ Å, $\beta = 109.85(2)°$, $Z = 4$) shows that the manganese atom displays a slightly distorted octahedral coordination being linked to three *facial* carbonyl ligands, to two nitrogen atoms of a bidentate 1,8-naphthyridine (η^2-naph) and to another nitrogen atom of a monodentate 1,8-naphthyridine (η^1-naph). A detailed variable temperature ^1H NMR study shows this structure persist in solution at low temperature. At higher temperature the complex is fluxional and there is a rapid exchange of the coordination modes of the two naph ligands: the bidentate becomes monodentate and the monodentate bidentate. The mechanism is intramolecular, the rate-limiting step being the opening of the four-membered ring formed by the metal and the η^2-naph.

1. Introduction

We have been interested recently in the coordination behaviour of potentially bidentate amine ligands and in the study of the fluxionality of the complexes they form when monodentate [1–5]. One of the most interesting ligands of this type is 1,8-naphthyridine (naph). With this ligand we have recently prepared the complexes [Mn(η^1-naph)(η^2-chel)$(CO)_3$]$^+$ [chel = *o*-phenanthroline (phen) or 2,2′-bipyridyl (bipy)] [4]. These two complexes are fluxional in solution with the metal atoms shuttling between the two nitrogen atoms of the η^1-naph in what can be called a 1,3-haptotropic shift [6]. An intramolecular concerted metal shift was proposed as the mechanism for this dynamic behaviour. In order to obtain more information on the fluxional behaviour of monodentate 1,8-naphthyridine we decided to prepare and study other complexes of manganese(I) with this ligand.

Correspondence to: Dr. J. Vinaixa.

2. Experimental section

2.1. General remarks

The reactions were carried out under dry dinitrogen or argon, using Schlenk tube techniques. Solvents were dried by appropriate methods and distilled under dinitrogen prior to use. Chemical analyses were carried out at the Institut de Química Bio-orgànica de Barcelona (C.S.I.C.). Conductivities of 10^{-4} M acetone solutions of the new compounds were measured with a Radiometer CMD3 conductivity bridge. Proton and $^{13}C\{^1H\}$ NMR spectra were obtained from acetone-d_6 solutions and were recorded on Brucker WP 80SY, equipped with a B-VT-1000 variable temperature unit and Varian XL 200 spectrometers; chemical shifts are referred to internal $SiMe_4$.

The 1,8-naphthyridine [7] and the complex [MnBr(naph)$(CO)_3$ [8] were prepared as previously described.

Safety note: Even though we have not had any problems using perchlorate salts and perchlorate complexes, it must be borne in mind that perchlorate salts

0022-328X/93/$6.00

of metal complexes with organic ligands are potentially explosive [9]. Great caution should therefore be exercised when handling these materials.

2.2. Preparation of $[Mn(naph)_2(CO)_3]ClO_4 \cdot C_4H_{10}O$ (1)

Method (a): a mixture of $[MnBr(naph)(CO)_3]$ (0.28 g, 1 mmol) and $AgClO_4$ (0.25 g, 1.2 mmol) in CH_2Cl_2 (15 ml) was stirred at room temperature for 2 h. The resulting solution of $[Mn(OClO_3)(naph)(CO)_3]$ was then filtered through Celite. 1,8-Naphthyridine (0.16 g, 1.2 mmol) was added to the solution, and after stirring at room temperature for 3 h, diethyl ether (50 ml) was added. The microcrystalline solid was filtered, washed with diethyl ether and hexane, and then vacuum dried. Yield *ca.* 60%.

Method (b): a mixture of $[MnBr(CO)_5]$ (0.28 g, 1 mmol) and $AgClO_4$ (0.25 g, 1.2 mmol) in CH_2Cl_2 (15 ml) was stirred at room temperature for 2 h. The resulting solution of $[Mn(OClO_3)(CO)_5]$ was then filtered through Celite. 1,8-Naphthyridine (0.30 g, 2.2 mmol) was added to the solution, and after stirring at room temperature for 3 h, diethyl ether was added. The precipitated solid was treated as in method (a). Yield *ca.* 73%; m.p. 160°C dec. Anal. Calc for $C_{23}H_{22}ClMnN_4O_8$: C, 47.45; H, 3.9; N, 9.8. Found: C, 47.7; H, 3.7; N, 9.9%. IR: ν_{max}(CO) 2045s, 1965sh, and 1955s cm^{-1} (CH_2Cl_2); L_M 149 Ω^{-1} cm^2 mol^{-1} (acetone). $^{13}C\{^1H\}$ NMR at 308 K, C_α: 157.7, C_β: 125.4, C_γ: 140.1 ppm.

2.3. Preparation of $[Mn(naph)(CO)_5]ClO_4$ (3)

A mixture of $[MnBr(CO)_5]$ (0.28 g, 1 mmol) and $AgClO_4$ (0.25 g, 1.2 mmol) in CH_2Cl_2 (15 ml) was stirred at room temperature for 2 h. The resulting solution of $[Mn(OClO_3)(CO)_5]$ was filtered through Celite, cooled to −80°C and acetone (to keep the manganese complex in solution) and a cooled solution of 1,8-naphthyridine (0.10 g, 0.75 mmol) in dichloromethane/diethylether (1:1) added. This solution was stirred at −80°C for 15 min, and cold (−80°C) diethylether (60 ml) was added. The product was isolated by evaporation of the solvents at ≈ −20°C, and vacuum dried. The product must be stored cold to avoid decomposition. Yield *ca.* 40%. Anal. Calc for $C_{13}H_6ClMnN_2O_9$: C, 36.8; H, 1.4; N, 6.6. Found: C, 36.6; H, 1.3; N, 6.8%. IR: ν_{max}(CO) 2160w, 2115vw, 2075s, and 2045m cm^{-1} (CH_2Cl_2).

2.4. Structure determination of fac-$[Mn(\eta^1\text{-naph})(\eta^2\text{-naph})(CO)_3]ClO_4 \cdot CH_2Cl_2$

A single crystal suitable for X-ray diffraction study was grown by cooling a saturated CH_2Cl_2 solution of $[Mn(\eta^1\text{-naph})(\eta^2\text{-naph})(CO)_3]ClO_4$ at −15°C for several weeks. The details of the crystal structure determination are given in Table 1. The structure was solved by a Patterson synthesis, using the MULTAN computer program and refined by the full-matrix least-squares method with the SHELX76 computer program. The function minimized was $\Sigma w[|F_o| - |F_c|]^2$, where $w = [\sigma^2(F_o) + 0.0009(F_o)^2]^{-1}$, f, f' and f'' were taken from the *International Tables of X-ray Crystallography*. The position of H atoms were computed and refined with an overall isotropic temperature factor.

TABLE 1. Crystallographic data for fac-$[Mn(\eta^1\text{-naph})(\eta^2\text{-naph})(CO)_3]ClO_4 \cdot CH_2Cl_2$

Chemical formula	$C_{19}H_{12}ClN_4O_7Mn \cdot CH_2Cl_2$
Formula weight	591.25
Space group	$P2_1/a$ (non-standard No. 14)
a	16.006(3) Å
b	12.024(2) Å
c	13.004(2) Å
β	109.85(2)°
V	2362(1) Å^3
Z	4
ρ_{calcd}	1.686 g cm^{-3}
λ(Mo Kα)	0.71069 Å
μ	9.82 cm^{-1}
$F(000)$	1208
T	15°C
Scan limits	$2° \le \theta \le 25°$
No. reflec. measured	2132
Observed refl. ($I > 2.5\sigma(I)$)	1957
$R(F_o)$	0.047
$R_w(F_o)$	0.049

3. Results and discussion

3.1. Preparation and characterization

The room temperature reaction between $[Mn(OClO_3)(CO)_5]$, prepared *in situ* from $[MnBr(CO)_5]$ and $AgClO_4$, and 1,8-naphthyridine, in a 1:2 molar ratio, gave rise to $[Mn(\eta^1\text{-naph})(\eta^2\text{-naph})(CO)_3]ClO_4$ (**1**). When the same reaction was carried out in a 1:1 molar ratio at a temperature between 0°C and room temperature a mixture of two naph complexes, **1** and $[Mn(\eta^2\text{-naph})(CO)_4]ClO_4$ (**2**), was observed in the ^1H NMR spectrum of a solution of the precipitated solid. When the reaction between the perchlorato-complex $[Mn(OClO_3)(CO)_5]$ and naph was carried out at −80°C in a 1:1 mol ratio, and the final product was isolated at ≈ −20°C the complex $[Mn(\eta^1\text{-naph})(CO)_5]ClO_4$ (**3**) was obtained. Complex **2** was converted into complex **1** by reaction with an excess of 1,8-naphthyridine. The variable temperature ^1H NMR spectra of the mixture in acetone showed that both aromatic rings of the heterocycle for complex **2** were equivalent between

35°C and −100°C. A mixture of complexes **1** and **2** showed, in the CO stretching region of the IR spectrum, two bands at 2120 and 1970 cm^{-1}. These arise neither from complex **1** nor from **3** but were almost in the same position as two of the four bands observed for $[Mn(\eta^2\text{-naph})(CO)_4]ClO_4$ [10] in the same region. Even though complex **2** was not isolated pure, the above observations suggest that it was clearly $[Mn(\eta^2\text{-naph})(CO)_4]ClO_4$.

Complex **1** can also be obtained by the room temperature reaction of $[Mn(OClO_3)(\eta^2\text{-naph})(CO)_3]$, prepared *in situ* from $[MnBr(\eta^2\text{-naph})(CO)_3]$ and $AgClO_4$, and naph in a 1:1 mol ratio.

All the new compounds are yellow solids, very soluble in acetone. Complexes **1** and **2** are air-stable in the solid state but in solution they must be kept under an inert atmosphere. Complex **3** decomposes at room temperature in the solid state as well as in solution. The decomposition of complex **3** was followed in acetone by variable temperature ^1H NMR spectroscopy (see below).

The analytical data for complex **1** and **3** are in accord with the proposed formulae. Crystals of the perchlorate salt of complex **1** exhibit a strong tendency to include solvent molecules. Thus, the crystals obtained for the X-ray study contained a molecule of CH_2Cl_2, and the solid precipitated by the addition of diethylether contained a molecule of this solvent in a 1:1 ratio. The presence of CH_2Cl_2 of solvation was confirmed by the X-ray study itself, and that of diethyl ether by characteristic resonances in the ^1H NMR spectrum in acetone-d_6 of appropriate intensity at 1.11 ppm (triplet) and 3.41 ppm (quartet) ($^3J = 7.0$ Hz). Conductivity measurements show that compound **1** is a 1:1 electrolyte in acetone. The decomposition of complex **3** in solution at room temperature is too rapid for the conductivity measurement to be of any real significance. The IR spectra of complexes **1** and **3** show bands due to all the ligands and to the perchlorate anion. The IR ν(CO) are in accord with the expected structures.

3.2. *Crystal structure of fac-[Mn(η^1-naph)(η^2-naph)(CO)$_3$]ClO$_4$·CH$_2$Cl$_2$*

The crystal structure of *fac*-$[Mn(\eta^1\text{-naph})(\eta^2\text{-naph})(CO)_3]ClO_4 \cdot CH_2Cl_2$ shows discrete ions and solvate molecules linked by Van der Waals' and ionic forces. Figure 1 shows a view of the complex ion, with the atom numbering.

Selected bond distances and angles are given in Table 2. Positional parameters for non-hydrogen atoms are listed in Table 3.

The manganese atom displays a distorted octahedral coordination, being linked to three nitrogen atoms of two 1,8-naphthyridine ligands, one bidentate and one monodentate, and tree carbon atoms of *fac* carbonyl ligands.

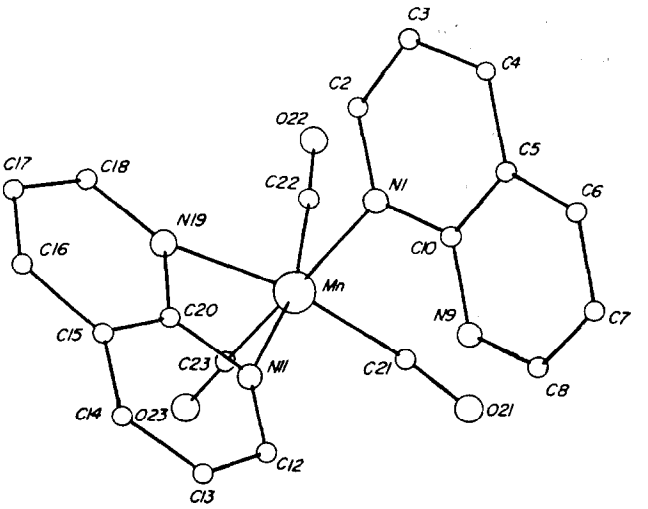

Fig. 1. Molecular structure of *fac*-$[Mn(\eta^1\text{-naph})(\eta^2\text{-naph})(CO)_3]ClO_4$ (**1**).

The Mn–N(η^2-naph) bond distances, [average 2.093(6) Å] are somewhat larger than the Mn–N (*o*-phenanthroline) bond distances found in octahedral complexes of Mn^I with carbonyl ligands *trans* to the amine such as *fac*-$[Mn(\eta^1\text{-naph})(\eta^2\text{-phen})(CO)_3]^+$ [average 2.06(1) Å] [4], $[\{fac\text{-}Mn(CO)_3(phen)\}_2(\mu$-

TABLE 2. Selected bond lengths (Å) and angles (deg) for $[Mn(\eta^1\text{-naph})(\eta^2\text{-naph})(CO)_3]ClO_4 \cdot CH_2Cl_2$ with standard deviations in parentheses.

Bond lengths			
N(9)–Mn	3.196(6)	C(12)–N(11)	1.309(8)
N(1)–Mn	2.116(5)	C(20)–N(11)	1.373(8)
N(11)–Mn	2.087(6)	N(19)–C(18)	1.335(8)
N(19)–Mn	2.099(6)	C(20)–N(19)	1.361(8)
C(21)–Mn	1.809(7)	O(21)–C(21)	1.138(7)
C(22)–Mn	1.803(9)	O(22)–C(22)	1.149(8)
C(23)–Mn	1.796(10)	O(23)–C(23)	1.155(9)
Bond angles			
N(11)–Mn–N(1)	88.1(2)	N(19)–Mn–N(1)	86.5(2)
N(19)–Mn–N(11)	64.1(2)	C(21)–Mn–N(1)	94.5(3)
C(21)–Mn–N(11)	100.3(3)	C(21)–Mn–N(19)	164.3(3)
C(22)–Mn–N(1)	90.3(3)	C(22)–Mn–N(11)	166.7(3)
C(22)–Mn–N(19)	102.6(3)	C(22)–Mn–C(21)	93.1(3)
C(23)–Mn–N(1)	177.7(3)	C(23)–Mn–N(11)	93.6(3)
C(23)–Mn–N(19)	93.0(3)	C(23)–Mn–C(21)	86.6(3)
C(23)–Mn–C(22)	87.7(4)	C(2)–N(1)–Mn	118.8(5)
C(10)–N(1)–Mn	124.0(5)	C(6)–C(5)–C(4)	122.3(8)
N(9)–C(10)–N(1)	115.2(6)	C(12)–N(11)–Mn	149.5(5)
C(20)–N(11)–Mn	93.7(4)	C(16)–C(15)–C(14)	127.9(8)
C(18)–N(19)–Mn	149.9(5)	C(20)–N(19)–Mn	93.5(4)
N(19)–C(20)–N(11)	108.6(6)	O(21)–C(21)–Mn	173.9(6)
O(22)–C(22)–Mn	177.4(7)	O(23)–C(23)–Mn	174.8(7)

TABLE 3. Positional parameters ($\times 10^4$) for non-hydrogen atoms with standard deviations in parentheses.

	x	y	z
Mn	89482(7)	12158(9)	77619(8)
H(1)	8239(4)	2623(4)	7992(5)
C(2)	8406(5)	3011(7)	8995(7)
C(3)	7963(10)	3920(15)	9261(16)
C(4)	7279(5)	4468(7)	8441(7)
C(5)	7099(5)	4074(6)	7372(6)
C(6)	6470(5)	4567(7)	6476(8)
C(7)	6307(5)	4160(7)	5464(8)
C(8)	6808(6)	3235(8)	5336(7)
H(9)	7424(4)	2725(5)	6143(5)
C(10)	7579(4)	3154(6)	7152(6)
N(11)	9337(3)	2153(5)	6651(4)
C(12)	9195(5)	2477(7)	5645(6)
C(13)	9752(6)	3247(7)	5371(7)
C(14)	10463(5)	3701(7)	6166(7)
C(15)	10635(4)	3366(6)	7257(6)
C(16)	11339(5)	3706(7)	8198(7)
C(17)	11408(5)	3267(7)	9188(7)
C(18)	10778(5)	2505(6)	9297(6)
N(19)	10096(4)	2178(4)	8432(5)
C(20)	10051(5)	2612(6)	7448(6)
C(21)	7982(5)	527(6)	6838(6)
O(21)	7423(3)	49(4)	6217(5)
C(22)	8827(5)	567(7)	8953(7)
O(22)	8782(4)	163(5)	9734(5)
C(23)	9562(5)	10(7)	7624(7)
O(23)	9902(4)	−813(6)	7533(6)
Cl(3)	6963(1)	−2183(2)	7820(2)
O(31)	6753(5)	−2870(5)	8607(5)
O(32)	6937(6)	−2816(6)	6911(6)
O(33)	7812(4)	−1753(7)	8307(6)
O(34)	6370(5)	−1291(6)	7495(6)
Cl(1)	8767(2)	5571(2)	6382(2)
Cl(2)	9647(2)	5591(3)	8729(2)
C	9223(8)	6389(10)	7513(9)

CN)]PF_6 [average 2.057(11) Å] [12], *cis-cis*-[Mn-$(CO)_2$(phen){CN[$C(CH_3)_3$]}{CN(C_6H_5)}]ClO_4 [average 2.061(9) Å] [13], and *fac*-[$Mn(CO)_3$(phen){CN-[$C(CH_3)_3$]}]ClO_4 [average 2.063(3) Å] [13]. This is attributed to a poorer overlap between the ligand and the metal orbitals due to the unfavourable orientation of the nitrogen lone pairs of 1,8-naphthyridine when compared with that in *o*-phenanthroline. The Mn–N(1) and the Mn–N(9) bond distances are very similar to the Mn-N(η^1-naph) and Mn-N(non-coordinated) bond distances found in *fac*-[Mn(η^1-naph)(η^2-phen)$(CO)_3$]$^+$ [2.112(7) and 3.299(7) Å] [4]. The large Mn–N(9) distance, together with the fact that there is very little distortion in the coordination of the η^1-naph [bond angle N(1)–Mn–C(23), 177.7(3)°], indicates that there is no interaction between the manganese and the farther nitrogen atom of the η^1-naph. The three Mn–CO bond lengths can be assumed equivalent [average 1.803(5) Å] and are typical for manganese(I) carbonyls [4,12,13].

The small chelate bite of the η^2-naph gives rise to a small N(11)–Mn-N(19) angle [64.1(2)°] and a lengthening of the remaining equatorial angles centred at Mn. A smaller distortion is observed in the bond angle opposite to the η^2-naph [bond angle C(22)–Mn–C(21), 93.1(3)°].

The effect of coordination of the 1,8-naphthyridine on the N–C–N [N(9)–C(10)–N(1) and N(19)–C(20)–N(11)] and on the opposite C–C–C [C(6)–C(5)–C(4) and C(16)–C(15)–C(14)] bond angles can be observed from the values of these bond angles in the free and coordinated 1,8-naphthyridine in several complexes listed in Table 4.

The decrease of the N–C–N bond angle in bidentate naph is likely to be due to a distortion of naph to optimize the overlap between the nitrogen lone pairs and the metal acceptor atomic orbitals, and the increase of the C–C–C bond angle to the rearrangement of the heterocycle. Table 4 suggests that, for an η^2-naph, decrease of coordination number is accompanied by a decrease in the N–C–N bond angle. This may be attributed to an increase of ionic character of the metal–naph interaction on going from Mn^I to Fe^{II} and then to Pr^{III}. A consequence would be a decrease in

TABLE 4. N–C–N(α) [a] and opposing C–C–C(β) [a] bond angles in 1,8-naphthyridines

Compound	N–C–N(α) (deg)	C–C–C(β) (deg)	reference
1,8-naphthyridine	115.3(2)	124.7(2)	16
cis-[PtCl(η^1-naph)$(PEt_3)_2$]$^+$	115.0(2)	124.0(2)	17
[Fe(η^2-naph)$_4$]$^{2+}$	111.6(1) [b]	126.1(1) [b]	18
[Pr(η^2-naph)$_6$]$^{3+}$	113.0(1) [b]	128.0(1) [b]	19
fac-[Mn(η^1-naph)(η^2-phen)$(CO)_3$]$^+$	114.5(7)	124.3(10)	4
fac-[Mn(naph)$_2(CO)_3$]$^+$			
(η^1-naph)	115.2(6)	122.3(8)	this work
(η^2-naph)	108.6(6)	127.9(8)	this work

[a] 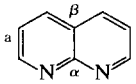 ; [b] Averaged values.

TABLE 5. Dihedral angles between most important planes of the complex *fac*-[Mn(η^1-naph)(η^2-naph)$(CO)_3$]$^+$ (1)

(equatorial)Plane A	MnN(11)N(19)C(21)C(22)			
(axial)Plane B	MnN(1)N(11)C(22)C(23)			
(axial)Plane C	MnN(1)N(19)C(21)C(23)			
(η^2-naph)Plane D	N(11)N(19)C(12)–C(20)			
(η^1-naph)Plane E	N(1)N(9)C(2)–C(8)			
Dihedral angles:	A/B 86.8°	A/C 89.2°	A/D 1.8°	A/E 88.4°
		B/C 76.9°	B/D 87.4°	B/E 50.2°
			C/D 87.4°	C/E 52.9°
				D/E 87.4°

the distortion of the N–C–N bond angle, required for better overlap between the ligand and metal orbitals. The most important planes of the molecule, and the dihedral angles between them, are listed in Table 5.

3.3. NMR spectra

The ^{1}H NMR parameters for the complexes **1–3** are listed in Table 6.

3.3.1. [Mn(naph)$(CO)_5$)]ClO_4 (3)

The ^{1}H NMR spectrum of this complex in acetone-d_6 at −50°C supports a formulation in which only one nitrogen atom of the naph interacts with the metal [1,4].

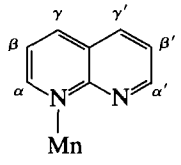

Warming of the sample to 0°C caused only small shifts of the resonances. At around 25°C another set of three doublets of doublets appeared in the spectrum. These new resonances were those of the naph ligands in complex **1** (see below). Above this temperature the velocity of decomposition of **3** into **1** speeded up. At 45°C the resonances of complex **3** broadened and, at the same time, several new resonances appeared in the heterocycle region of the spectrum (the most intense of the new resonances that appear above 45°C coincide with those of complex **2**). Above 45°C the resonances of **3** had completely disappeared and those of the decomposition products had increased in intensity. According to these results the bimolecular reaction that produces **1** from **3** is of lower activation energy than any other decomposition reaction, lower even than that for the displacement of a carbonyl by the non-coordinated nitrogen atom of the η^1-naph to produce [Mn(η^2-naph)$(CO)_4$]$^+$ [4]. The broadening of the resonances of complex **3** at 45°C is taken as indicating that the system is just entering into the coalescence region for the 1,3-haptotropic shift. For this process the mechanism previously proposed for [Mn(naph)(chel)$(CO)_3$]$^+$ [4] is likely to be operative.

If the system really is entering the coalescence region at 45°C, a lower limit of 66 kJ/mol is estimated for the energy barrier for the 1,3-haptotropic shift (derived from the equation $\Delta G^{\#} = 2.303RT_c(10.319 - \log k' + \log T_c)$ where T_c is the coalescence temperature, $k' = \pi(\Delta\nu)/2^{1/2}$ and $\Delta\nu$ is the frequency separation of the coalescing peaks, although the equation is strictly valid only for coalescence of two singlets [22]). This approximate value is consistent with our prediction [2] that for octahedral complexes of first row transition metals with an η^1-naph, $\Delta G^{\#}$ for the intramolecular 1,3-haptotropic shift should increase in the order Cr^0 {[Cr(naph)$(CO)_5$], 58.7 kJ/mol} [21] > Mn^I {[Mn(naph)$(CO)_5$]$^+$, > 66 kJ/mol} > Fe^{II} {[Fe(naph)$(CO)_2$Cp], ≫ 71 kJ/mol} [1]. Although the $\Delta G^{\#}$ values reported for the Mn^I and the Fe^{II}-complexes are lower limit values, no sign of exchange has been

TABLE 6. ^{1}H NMR spectra of 1,8-naphthyridine, free and as a ligand in complexes **1**, **2** and **3** [a]

Compound	Temperature (K)		Chemical shifts, ppm [b]			Coupling constant, Hz [b]		
			α α'	β β'	γ γ'	αβ α'β'	αγ α'γ'	βγ β'γ'
1,8-naphthyridine	308		8.97	7.47	8.28	4.1	2.0	8.2
1	185	η^1-naph	10.03	8.00	8.72	–	–	–
			9.56			–	–	–
		η^2-naph	9.86	8.00	8.72	–	–	–
	296		9.63	7.83	8.60	4.7	1.7	8.4
2	308		9.42	8.06	8.89	4.6	1.5	8.2
3	296		9.88	7.97	8.95	5.5	1.5	7.9
			9.39	7.98	8.79	4.35	1.8	8.2

[a] In acetone-d_6. [b] α, β, and γ position are labelled relative to the nitrogen atoms. Unprimed positions are adjacent to the coordinated nitrogen and primed positions are adjacent to the non-coordinated nitrogen (see structure in the text, 3.3.1.).

observed for the Fe^{II} complex even at the highest temperature studied, whereas for the Mn^I complex at least some line broadening of the NMR resonances due to exchange has been observed.

The $\Delta G^{\#}$ value for $[Mn(\eta^1\text{-naph})(CO)_5]^+$ is higher than that for *fac*-$[Mn(\eta^1\text{-naph})(\eta^2\text{-chel})(CO)_3]^+$ (63 kJ/mol) [4], possibly due to the greater electronegativity of the manganese atom in complex **3** than in $[Mn(naph)(chel)(CO)_3]^+$, due to the two electron-withdrawing ligands in the former carbonyls rather than two electron donors in the latter (the two nitrogen atoms of the chelating ligand). According to our calculations with model systems, an increase in the Mn^I electronegativity should produce a higher energy barrier [2].

3.3.2. *[Mn(η¹-naph)(η²-naph)(CO)₃]ClO₄ (1)*

The variable temperature ^1H and $^{13}C\{^1H\}$ NMR spectra of this complex in acetone-d_6 are shown in Figs. 2 and 3, respectively.

3.4. *^1H NMR spectra*

Below −88°C freezing spoiled the experiment. This set of spectra can be interpreted readily assuming that there is a dynamic process that renders both 1,8-naphthyridine ligands equivalent. Thus, at low temperature the structure of the complex in solution is the same as that in the solid state, an octahedral Mn^I complex of *fac* geometry with one η^1-naph and one η^2-naph. At −88°C the slow exchange limit had not been reached yet, and the β and γ resonances of the η^1-naph and η^2-naph were not resolved, but the α resonances, more affected by the coordination to the metal, appeared as three broad singlets. The one with greater intensity was assigned to the equivalent α protons of the η^2-naph while the other two resonances were assigned to the two non-equivalent α protons of the η^1-naph.

The assignment of these resonances to coordinated (α) and non-coordinated (α') rings has been done on the basis of their chemical shifts. For a monodentate 1,8-naphthyridine the resonance of the α'-proton is expected at higher field than that of the α-proton as observed for most complexes with a monodentate naph: *cis*-$[PtCl(\eta^1\text{-naph})L_2]^+$ (L = PEt_3 or PMe_2Ph) [20], $[M(CO)_5(\eta^1\text{-naph})]$ (M = Cr or W) [21], $[CpFe(CO)_2(\eta^1\text{-naph})]^+$ [1]. Nevertheless, for at least three complexes with a monodentate 1,8-naphthyridine the α-proton resonance has been found at higher field than that of the α'-proton: *cis*-$[PtCl(\eta^1\text{-naph})(PPh_3)_2]^+$ [20], and *fac*-$[Mn(\eta^1\text{-naph})(\eta^2\text{-chel})(CO)_3]^+$ (chel = phen or bipy) [4]. This anomalous behaviour in the latter two complexes has been attributed to a ring-current shielding effect affecting the α-proton more than the α'. The similarity of those two manganese(I) complexes with

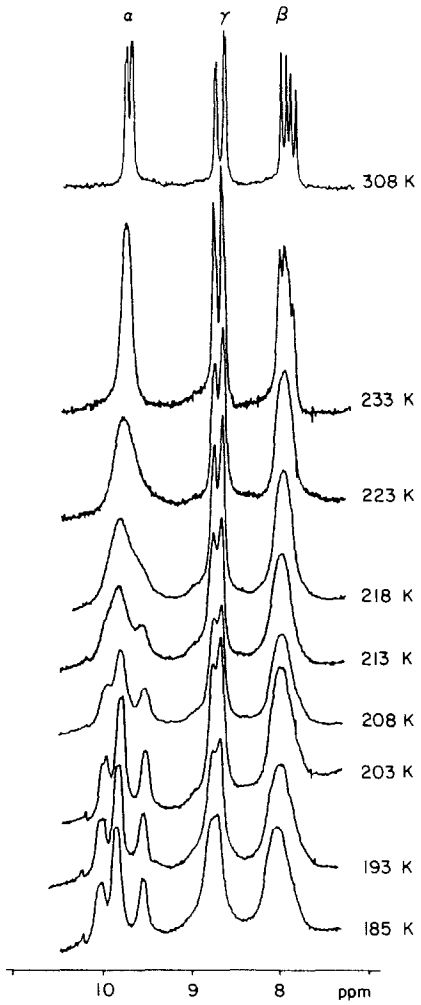

Fig. 2. 80 MHz variable temperature ^1H NMR spectra of *fac*-$[Mn(\eta^1\text{-naph})(\eta^2\text{-naph})(CO)_3]ClO_4$ (**1**) in acetone-d_6. The peaks labelled α, β, and γ denote positions with respect to nitrogen atoms.

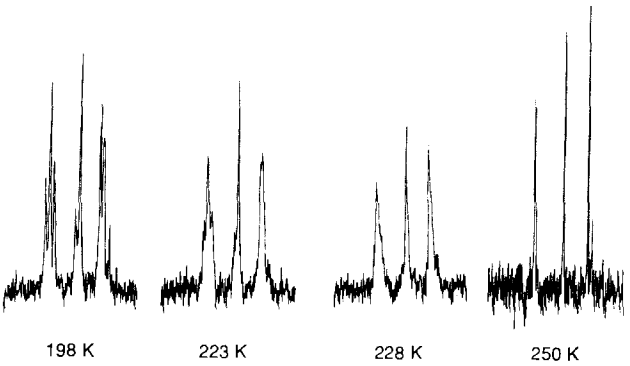

Fig. 3. 20.1 MHz variable temperature ^{13}C NMR spectra of the α-carbon of the naph of *fac*-$[Mn(\eta^1\text{-naph})(\eta^2\text{-naph})(CO)_3]ClO_4$ (**1**) in acetone-d_6.

complex **1** would allow us to make a similar assignment for the α and α' resonances of this complex. However, for no complex with a monodentate naph has the α'-proton resonance ever been observed higher than 9.5 ppm, whereas the α-proton resonance has been observed around 10 ppm for two complexes: [W(η^1-naph)$(CO)_5$] (10.08 ppm) [21], and [CpFe(η^1-naph)$(CO)_3]^+$ (9.89 ppm) [1]. Therefore we assign the resonance at 10.0 ppm to the α-proton and that at 9.56 ppm to the α'-proton.

3.5. $^{13}C\{^1H\}$ NMR spectra

The α-carbon resonances of the naph ligands in *fac*-[Mn(η^1-naph)(η^2-naph)$(CO)_3$]ClO_4 appear as a pseudotriplet that collapses to a singlet above 258 K. This is consistent with the variable-temperature ^1H NMR study and the crystal structure determination. The two resonances of lower intensity, at 155.8 and 161.0 ppm, are assigned to the α-carbons of the monodentate naph and the other, at 158.3 ppm and of double intensity, to the two equivalent α-carbons of the bidentate naphthyridine.

The coalescence of both the three α-proton and the three α-carbon resonances at high temperature shows that the two naph ligands exchange their coordination modes: the monodentate naphthyridine becomes bidentate and the bidentate becomes monodentate, and become equivalent. As a consequence of this process the manganese atom exchanges the nitrogen atom of the η^1-naph to which it is coordinated.

3.6. Mechanism of the fluxional process of complex 1

In order to obtain information on the fluxional process two different experiments were undertaken. First the ^1H NMR spectrum of an acetone-d_6 solution of complex **1** at 193 K was obtained and no changes were observed when the sample was diluted first to a half and then to a quarter of the initial concentration. In the second experiment naph was added to a solution of complex **1** in acetone-d_6 and its ^1H NMR spectra at 193 K was obtained: apart from the appearance of the resonances of the free naph, no changes in the spectrum were observed. On raising the temperature to 308 K the resonances of the coordinated naph remained well resolved and not affected by the presence of free naph. These experiments showed that the fluxional process was unimolecular.

Treating the two separate α-proton bands of the monodentate naph at 9.56 and 10.03 ppm (185 K) as singlets which coalesce with T_c *ca.* 215 K, a rough estimate of 44 kJ/mol for the energy barrier for the process is obtained. The same value is obtained when the two α-carbon resonances of the monodentate naphthyridine at 160.7 and 155.5 ppm are treated as two coalescing singlets at 225 K ($\Delta G^{\#} = 44.4$ kJ/mol). The calculation is possible since the other two α-protons, or α-carbons, of the bidentate ligand have the same chemical shift, nearly the value of the final average of all α-protons (α-carbons). The activation energy for the fluxional process of **1** is much lower than that obtained for the 1,3-haptotropic shift in [Mn(η^1-naph)(η^2-chel)$(CO)_3]^+$ (chel = phen or bipy) [4], ($\Delta G^{\#} = 63$ kJ/mol).

Were **1** and [Mn(η^1-naph)(η^2-naph)$(CO)_3]^+$ to react by the same mechanism a similar activation energy would be expected and this is obviously not in accord with experiment. The mechanism, that could be called associative, operative in the complex [Mn(η^1-naph)(η^2-chel)$(CO)_3]^+$ [4], involving a seven-coordinate transition state formed by coordination of the non-coordinated nitrogen atom of the η^1-naph, does not explain the fluxional behaviour of complex **1**. The mechanism we proposed is one that could be called dissociative, involving a five-coordinate transition state formed by dissociation of one of the two coordinated nitrogen atoms of the η^2-naph. Coordination of any of the two non-coordinated naphthyridine nitrogen atoms to this coordinatively unsaturated transition state is equally probable and would result either in the exchange of coordination modes of the two naph ligands or in a 1,3-haptotropic shift.

This mechanism does not need to be completely dissociative but could very well be a concerted process, provided that dissociation is energetically the most important step.

4. Supplementary material available

A table listing the crystal data collection and refinement (2 pages); tables of anisotropic thermal parameters and final hydrogen coordinates (2 pages); complete tables of bond lengths and angles (hydrogen and non-hydrogen atoms), and most important least-squares planes and deviations therefrom are available from the Cambridge Crystallographic Data Centre (6 pages); a listing of observed and calculated structure factors (9 pages) is also available from the authors.

References

1 M.J. Bermejo, B. Martinez and J. Vinaixa, *J. Organomet. Chem., 304* (1986) 207.
2 S. Alvarez, M.J. Bermejo and J. Vinaixa, *J. Am. Chem. Soc., 109* (1987) 5316.
3 M.J. Bermejo, J.I. Ruiz and J. Vinaixa, *Transition Met. Chem., 12* (1987) 245.
4 M.J. Bermejo, J.I. Ruiz, X. Solans and J. Vinaixa, *Inorg. Chem., 27* (1988) 4385.
5 M.J. Bermejo, J. Vinaixa, A. Pidcock and I.W. Nowell, to be published.

6 N.T. Anh, M. Elian and R. Hoffmann, *J. Am. Chem. Soc., 100* (1978) 110; T.A. Albright, P. Hofmann, R. Hoffmann, C.P. Lillya and P.A. Dobos, *J. Am. Chem. Soc., 105* (1983) 3396.
7 W.W. Paudler and T.J. Kress, *J. Org. Chem., 32* (1967) 832.
8 J.R. Wagner and D.G. Hendricker, *J. Inorg. Nucl. Chem., 37* (1975) 1375.
9 W.C. Wooley, *J. Chem. Educ., 50* (1973) A335, and references therein.
10 R. Usón, V. Riera, J. Gimeno and M. Laguna, *Transition Met. Chem., 2* (1977) 123.
11 (a) D. Drew, D.J. Darensbourg and M.Y. Darensbourg, *Inorg. Chem., 14* (1977) 1579; (b) R. Usón, V. Riera, J. Gimeno, M. Laguna and M.P. Gamasa, *J. Chem. Soc., Dalton Trans.*, (1979) 996.
12 G.A. Carriedo, M.C. Crespo, V. Riera, M.L. Valin, D. Moreiras and X. Solans, *Inorg. Chim. Acta, 121* (1986) 191.
13 (a) M.L. Valin, D. Moreiras, X. Solans, M. Font-Altaba, X. Solans, F.J. García-Alonso, V. Riera and M. Vivanco, *Acta Crystallogr., Sect. C, 41* (1985) 1312; (b) M.L. Valin, D. Moreiras, X. Solans, M. Font-Altaba, F.J. García-Alonso, *Acta Crystallogr. Sect. C, 42* (1986) 417.
14 F.A. Cotton and D.C. Richardson, *Inorg. Chem., 5* (1966) 1851.
15 R.C. Little and R.J. Doedens, *Inorg. Chem., 12* (1973) 844.
16 A. Clearfield, M.J. Sims and P. Singh, *Acta Crystallogr., Sect. B, 28* (1972) 350.
17 G.W. Bushnell, K.R. Dixon and M.A. Khan, *Can. J. Chem., 56* (1978) 450.
18 (a) A. Clearfield, P. Singh, I. Bernal, *J. Chem. Soc., Chem. Commun.*, (1970) 389; (b) P. Singh, A. Clearfield and I. Bernal, *J. Coord. Chem., 1* (1971) 29.
19 A. Clearfield, R. Gopal and R.W. Olsen, *Inorg. Chem., 16* (1977) 911.
20 K.R. Dixon, *Inorg. Chem., 16* (1977) 2618.
21 K.R. Dixon, D.T. Eadie and S.R. Stobart, *Inorg. Chem., 21* (1982) 4318.
22 I.C. Calder and P.J. Garrat, *J. Chem. Soc. B*, (1967) 660.